

3D GRAIN RECONSTRUCTION FROM BOXSCAN DATA

A. Lyckegaard*, A. Alpers*, W. Ludwig[†], R.W. Fonda[‡], L. Margulies[§], A. Götz[†], H.O. Sørensen[¶], S.R. Dey^{||}, H.F. Poulsen* and E. M. Lauridsen*

* Center for Fundamental Research: Metal Structures in Four Dimensions, Materials Research Division, Risø-DTU, DK-4000 Roskilde, Denmark

[†] European Synchrotron Radiation Facility, BP220, 38043 Grenoble, France

[‡] Naval Research Laboratory, Code 6356, 4555 Overlook Avenue, SW, Washington, DC 20375, USA

[§] National Synchrotron Light Source II, Brookhaven National Laboratory, Upton, NY 11973-5000, USA

[¶] Department of Chemistry, University of Copenhagen, DK-2100 Copenhagen Ø, Denmark

^{||} Institute of Materials, Faculty of Mechanical Engineering, Ruhr-University Bochum, D-44801 Bochum, Germany

ABSTRACT

A method for reconstructing the 3D shape of a single grain in a polycrystal from far-field diffraction data is presented. The reconstruction is performed using an iterative algorithm, algebraic reconstruction technique (ART), to solve a linear system of equations obtained from data from the Boxscan technique. The Boxscan technique is a 3D X-ray diffraction-type scanning technique, which – in geometric tomography terms – provides 2-dimensional X-rays of the object as data. In this paper, we report on the first experimental 3D grain shape reconstruction based on a beta-titanium sample. By comparing our results to high-resolution phase contrast tomography, we find that the average error on the position of the grain boundary in this sample is 2.7 micrometers for a grain radius of 17 micrometers. This result is similar to other current methods.

1. INTRODUCTION

The last decades development of nondestructive 3D characterization techniques for polycrystals has been important in the field of materials science. The outcome of such a characterization could be a map of the positions of the grain centers in 3D or even better: a full

3D description of the topology in the volume (which is usually called a 3D grain map).

Within the general approach of 3-Dimensional X-Ray Diffraction (3DXRD) several grain mapping techniques have been explored. In the first one developed (Lauridsen, Schmidt, Suter and Poulsen 2001; Poulsen 2004) the sample is illuminated layer-by-layer with a line-shaped high-energy X-ray beam and the diffracted signal is recorded on both a near-field and a far-field detector as the sample is rotated. Where the far-field signal gives information for resolving the grain orientation, the near-field detector shows a 2D projection of the diffracting grains in the illuminated sample layer. As shown in Poulsen and Fu (2003) and Fu, Knudsen, Poulsen, Herman, Carvalho and Liao (2006) applying algebraic reconstruction techniques (ART) to the near-field signal enables the possibility to produce spacefilling grain maps of the illuminated sample layer.

Ideas from 3DXRD and absorption tomography imaging triggered the development of Diffraction Contrast Tomography (DCT) (Ludwig, Schmidt, Lauridsen and Poulsen 2008; Johnson, King, Honnicke, Marrow and Ludwig 2008; Ludwig, Reischig, King, Herbig, Lauridsen, Johnson, Marrow and Buffiere 2009). While the sample is illuminated layer-by-layer in the methods mentioned above, DCT illuminates the entire volume of interest and records the absorption and the diffraction signal on the same detector positioned in the near-field as the sample is rotated. Again, the detector images show 2D projections of the diffracting grains for different rotation angles. By applying a set of criteria based on the geometry and the diffraction angles it is possible to determine the 2D projections associated with each grain. The 3D shape of the grain is computed from the 2D projections using ART. The use of data back projection is common to the 3DXRD and DCT making both methods sensitive to spot overlap on the detector.

High Energy X-ray Diffraction Microscopy (HEDM) (Suter, Hennessy, Xiao and Lienert 2006), and the methods presented in Alpers, Poulsen, Knudsen and Herman (2006) are variants of the 3DXRD but the grain maps are reconstructed by forward simulating candidate-solutions in a Monte Carlo optimization scheme. The problems with spot overlap are overcome, but powerful computer clusters might be necessary for the methods to be useful in practice.

The spatial resolutions of the methods discussed above are dependent on the pixel size of the detector and the methods require a detector placed close (1-10 mm) to the sample. Such detector positioning is in some cases prohibited due to the presence of spacious experimental equipment, e.g. a furnace or a stress rig. In this case only a far-field detector can be used. With only a far-field detector in the set-up, with 3DXRD one could obtain information on the crystallography, stress-state, volume and center of mass of more than 1000 grains (Oddershede, Schmidt, Poulsen, Sørensen, Wright and Reimers 2010). However, the spatial resolution is reduced to approximately 10 micrometers and no shape information is available. Yet the combination of position and volume makes it possible to generate approximate grain maps based on a Laguerre tessellation (Lyckegaard, Lauridsen, Ludwig, Fonda and Poulsen 2010). Laguerre tessellations are extensions of the Voronoi tessellation and are found to provide a better approximation to the underlying grain structure.

In the techniques discussed above, the limiting factor has been the detector resolution. Where the detectors have resolutions in the range of micrometers, the scanning mechanics has sub-micrometer resolution, some even down to 10s of nanometers. Thus, using the mechanics to probe the sample by translating vertically and horizontally through an extended line beam while recording the diffracted X-rays on a far-field detector could overcome the problem of limited detector resolution. A technique based on this principle has been developed through the Boxscan technique (Lyckegaard, Poulsen, Ludwig, Fonda, Margulies, Götz, Sørensen, Dey and Lauridsen 2010). The Boxscan technique is a variant of 3DXRD, but uses only a far-field detector. It is a scanning technique where two datasets are acquired: one where the sample is scanned vertically and one where it is scanned horizontally.

By combining the two datasets and using the knowledge on the diffracting angles and the geometry, the size and the positions of the grain centers in the sample can be determined with high precision. In addition to this, several projections (2D X-rays in terms of geometric tomography) of the individual grains are obtained. As before, the position of the grain center and the size enables the construction of a grain map using a Laguerre tessellation. In this paper we point out that boxscan data comprise additional information, namely 1D profiles of the grain shapes. We discuss how to exploit this information and report on the first successful 3D grain shape reconstruction directly from Boxscan data (without the use of a tessellation).

2. BOXSCAN TECHNIQUE

2.1 Experimental setup. The experimental setup for the Boxscan technique is sketched in figure 1. The sample is mounted on top of a rotation stage ω and a set of stages for translations in x, y, z (laboratory coordinatesystem). ω rotates around the z -axis. The incoming focused X-ray beam is dimensioned by the motorized slits located in front of the sample. The diffracted X-rays are recorded by a 2D detector located in the far-field, i.e. no spatial information of the grain shape is recorded.

It is convenient to introduce a sample coordinatesystem (x_s, y_s, z_s) which is fixed to the sample, thus its rotation with respect to the laboratory coordinatesystem (x, y, z) is ω . For $\omega = 0$, (x_s, y_s, z_s) and (x, y, z) coincide. Eventually, the grain positions will be expressed in the sample coordinate system.

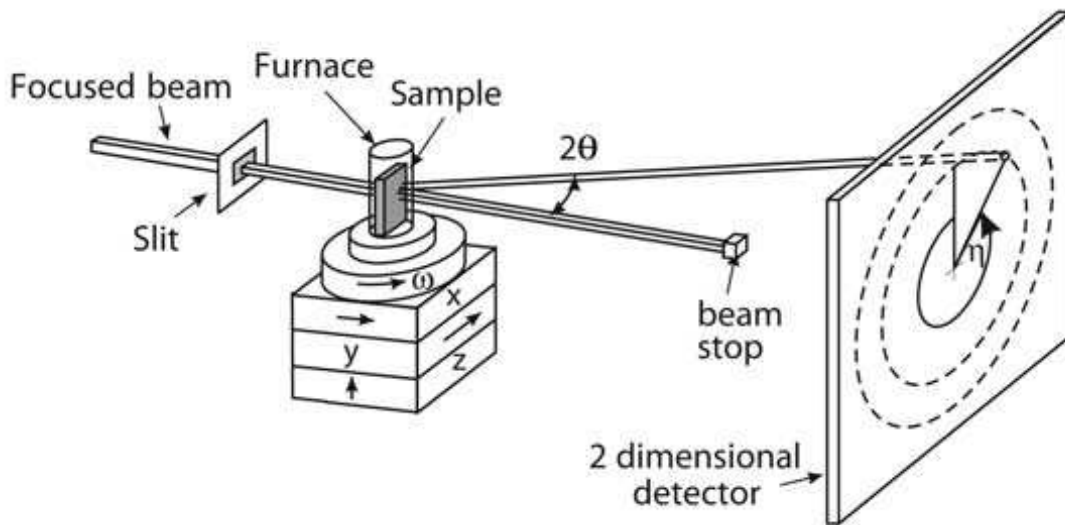


Fig. 1: Experimental setup of the Boxscan technique with definition of angles 2θ , ω and η .

2.2 Data acquisition. The data acquisition consists of two parts, one where the sample is translated vertically in z and one where it is translated horizontally in y . In the first case, the beam is slit down vertically to a horizontal line beam. For each vertical translation $z = z_1 \dots z_c$, a set of detector images are recorded for a series of sample rotations $\omega = \omega_1 \dots \omega_a$. In the second case, the beam is slit down horizontally to a vertical line beam. For each horizontal translation $y = y_1 \dots y_b$, a set of detector images are recorded for the same series of sample rotations $\omega = \omega_1 \dots \omega_a$.

2.3 Data analysis. The diffraction spots are extracted from the images and the values $(\omega, 2\theta, \eta,$

z) or $(\omega, 2\theta, \eta, y)$ of the diffraction angle and the vertical or horizontal translations are stored in a database. The subsets of diffraction spots with similar values $(\omega, 2\theta, \eta)$ and neighbouring values in y or z are denoted a profile, see figure 2. Each profile corresponds to the projection of the diffracting grain's shape onto the axis of translation in the laboratory coordinate system. Likewise, the intensity weighted average of the profile is the grains centre of mass on the axis of translation in the laboratory coordinate system, $y_{cms}(\omega)$ or $z_{cms}(\omega)$, for the given ω -value. It should be stressed here that the grain positions are fixed in the sample coordinate system but moves as a function of ω in the laboratory coordinate system. Each profile and the value $(\omega, 2\theta, \eta, y_{cms}(\omega))$ or $(\omega, 2\theta, \eta, z_{cms}(\omega))$ is stored in the database. Combining a horizontal with a vertical profile, $(\omega, 2\theta, \eta, y_{cms}(\omega))$ and $(\omega, 2\theta, \eta, z_{cms}(\omega))$, where $(\omega, 2\theta, \eta)$ are the same, i.e. from the same grain, gives a set of matches $(\omega, 2\theta, \eta, y_{cms}(\omega), z_{cms}(\omega))$ which can be used for indexing the grains in the dataset.

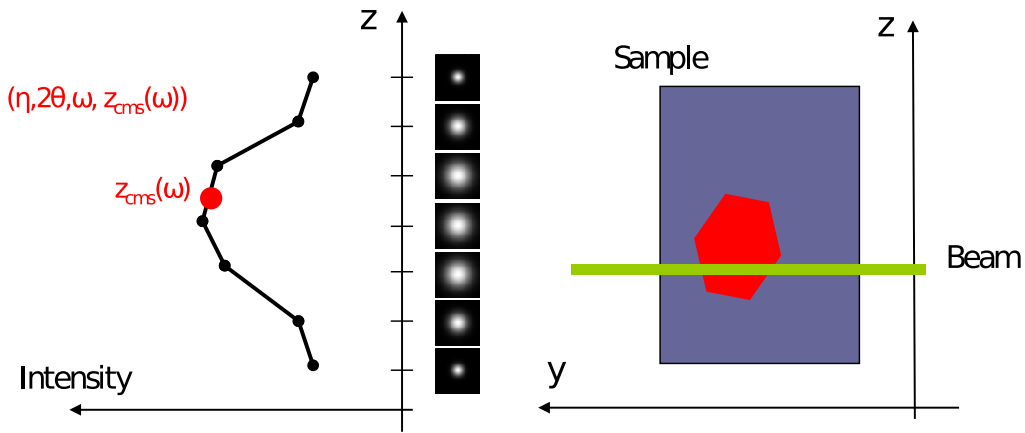


Fig. 2: Generation of vertical profile for one diffraction spot. As the sample is translated with respect to the beam (right) the diffraction spot changes appearance (middle). The profile is defined as the integrated intensity in the spot as function of z (left).

2.4 Indexing. For each match, the value $(\omega, y_{cms}(\omega), z_{cms}(\omega))$ maps to a line parallel to the (x_s, y_s) -plane in the 3D sample coordinate system and $(\omega, 2\theta, \eta)$ maps to a line in 3D orientation space, represented by Rodrigues vectors (for a definition of Rodrigues space see e.g. Morawiec and Field (1996)). A subset of the matches which fulfils $z_{cms}(\omega) = z_0 \pm \Delta z$ are extracted from the database and the intersection points (x_s, y_s, z_s) in the sample coordinate system and (r_1, r_2, r_3) in Rodrigues space for all possible combination of two matches in the subset are computed. If the intersection point (x_s, y_s, z_s) is inside the scanned volume and both exist in the Rodrigues space and is inside the fundamental zone, it is accepted and added to a list of 6D points $(x_s, y_s, z_s, r_1, r_2, r_3)$ for the subset. Now, by definition each grains centre of mass and crystallographic orientation is described by a single point in the 6D space $(x_s, y_s, z_s, r_1, r_2, r_3)$. Two matches from the same grain will intersect in exactly this point, thus the set of 6D points for the subset will have a high density of points where a grain possibly resides in 6D. To find grain candidates in the set of 6D points, a k-nearest neighbours search is performed. Points in 6D with high density are simulated and compared with the measured data. If there is agreement between the simulated grain candidates and measured data, the grain candidate is accepted as a grain.

2.5 Verification. The Boxscan technique was applied to a cylindrical beta titanium sample (300 micrometers in diameter) with an average grain size of 25 micrometers. The sample was scanned in a vertical range of 150 micrometers with a step size of $\delta_z = 4$ micrometers

and in a horizontal range of 330 micrometers with a step size of $\delta_y = 5$ micrometers. The beam had a vertical size of 20 micrometers for translations in z and a horizontal size of 30 micrometers for translations in y . The sample was probed in ω in two perpendicular 30 degrees intervals. The experimental setup used prohibited scanning the full horizontal width of the sample, allowing only a diamond shaped region inside the sample to be analysed.

In order to validate the grain centers determined by the Boxscan technique, they were compared to grain centers derived from a phase contrast tomography scan (PCT) of the same sample (Cloetens, Ludwig, Baruchel, Guigay, Pernot-Rejmankova, Salome-Pateyron, Schlenker, Buffiere, Maire and Peix 1999). The grains in the imaged volume were segmented by a series of image processing steps. First the grain boundaries were enhanced and noise suppressed by correlating with a model of a grain boundary. After this followed a binarization, Euclidean distance transform and a watershedding. After the binarization a few manual corrections were needed to segment the grains correctly.

The grain centers were computed for the grains found from PCT and compared to the ones from the Boxscan technique. The Boxscan technique determined 133 of 159 verification grains correctly. The grain that were not found were either on the limit of the scanned region or very small grains. The error on the grains centers was 2.6 micrometers, i.e. the precision of the grain centers were better than the step sizes $\delta_z = 4$ micrometers and $\delta_y = 5$ micrometers.

3. APPLICATION OF ALGEBRAIC RECONSTRUCTION TECHNIQUE TO BOXSCAN DATA

The algebraic reconstruction technique (ART) as described by Kak and Slaney (1988) is a framework for solving m linear equations in n unknowns $\mathbf{Ax} = \mathbf{b}$, with dimensions $\mathbf{A}_{m \times n}$, $\mathbf{x}_{n \times 1}$, $\mathbf{b}_{m \times 1}$. In the random version of ART, we iteratively produce solutions \mathbf{x}_{k+1} by projecting the current solution \mathbf{x}_k onto a random row of the \mathbf{A} -matrix:

$$\mathbf{x}_{k+1} = \mathbf{x}_k + \lambda \frac{\mathbf{b}_i - \mathbf{a}_i \mathbf{x}_k}{\|\mathbf{a}_i\|^2} \mathbf{a}_i \quad (1)$$

where \mathbf{a}_i correspond to the i th row of the \mathbf{A} -matrix and λ is a relaxation parameter.

The Boxscan technique gives shape information of the individual grains through the profiles. For a point (t, I) in a profile, where I is the measured intensity and t is a position in y or z , I scales linearly with the integral of the grain volume which the beam illuminated at position t . The beam positions y and z and the beam widths are known, hence it is possible to set up a system of linear equations by subdividing the sample space (x, y, z) into n voxels. The voxels in the subdivided sample space are given a weight between 0 and 1 according to the fraction of the voxel that is illuminated by the beam and placed into the \mathbf{A} -matrix as a row. Similarly, I is stored in the same row index of the \mathbf{b} -vector. This is repeated for all beam positions in all profiles belonging to one grain. The unknown \mathbf{x} -vector holds the intensity of the voxels and will for a correct solution give a 3D description of the grain.

Assuming that the resolution is such that we can assume that the voxels are either completely void or filled by a grain, it is natural to consider \mathbf{x} -vectors that are either 0- or 1-valued. ART, however, typically returns solutions \mathbf{x} that are real valued, and not necessarily binary. A common way to overcome this problem is to introduce a threshold. In the following, we find a suitable threshold value by using the knowledge obtainable from the profiles. Since each profile is a projection of the grain volume, it is possible to estimate the grain radius from the profiles belonging to a grain. With a sphere as grain model, a projection of the grain convoluted with the beam profile can be fitted to all profiles in a grain. The average

of all the fitted sphere radii is used for calculating the grain volume, which is used to set the threshold on the ART solution such that the volume of the binarized ART solution is equal to the estimated grain volume.

4. RESULTS

For the chosen grain in the Boxscan dataset, the sample space was voxelized with a voxel size of 2 micrometers. This in conjunction with voxel weights and profiles was used to generate the linear system $\mathbf{Ax} = \mathbf{b}$. The system had 15625 unknowns and 931 equations making it an under-determined system. The ART algorithm was run with $\lambda = 10^{-5}$ and terminated when the figure of merit $\|\mathbf{Ax} - \mathbf{b}\|/\|\mathbf{b}\|$ had converged. The average grain radius was estimated to 17 micrometers and the corresponding threshold was set as described above. In figure 3 the reconstructed binarized grain is compared to the same grain segmented from the PCT verification data resampled to a 2 micrometers resolution.

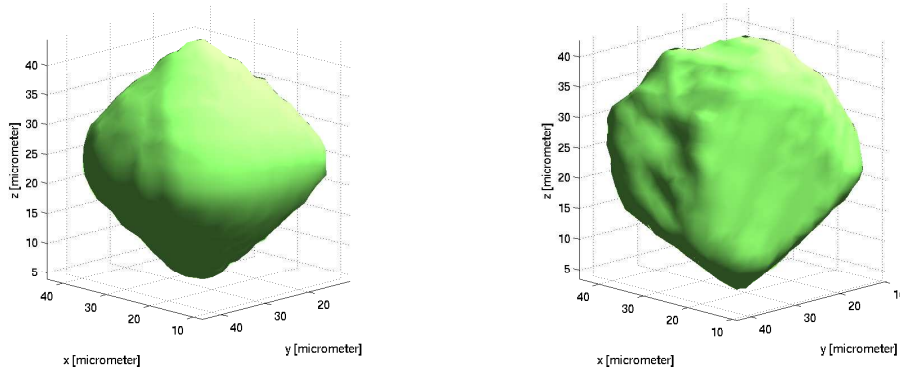


Fig. 3: Left: 3D grain shape found with ART. Right: 3D grain shape from verification data. The units on the axes are micrometers.

The grain reconstructed with ART is not as detailed as the verification data but the overall shape is caught. The ART solution labels 87% of the voxels in the verification data correctly. For a better comparison of the ART solution to the verification data, the distance between the grain boundaries of the two grains are mapped onto the surface of the grain from the verification data, see figure 4, left. As the figure shows, the smooth ART solution is not capable of reconstructing areas around corners. The average distance between the two grain boundaries is 2.7 micrometers. Figure 4, right, shows a single layer of the two grains where red is verification data, green Boxscan data and yellow is overlap. Again it is possible to see that the ART solution has a smoother and more rounded shape than the verification data.

5. DISCUSSION

As laid out in the introduction, the question to be answered was if additional projection information could improve the 3D grain shape reconstructions. Based on the Laguerre tessellation approach, in Lyckegaard et al. (2010a) the number of correctly assigned voxels was measured to be 86% for a sample similar to the one used here. The 86% was measured as an average over all grains where the grain neighbour relationship was known. In our case

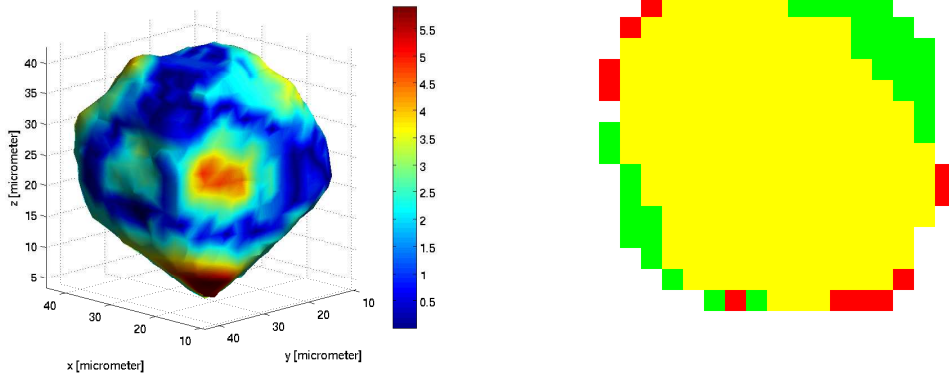


Fig. 4: Left: Distance between the grain boundaries of the ART reconstruction and the verification data for the morphology of the same grain. The colour scale is in units of micrometers. Right: A superposition of the same layer in the two reconstructions of the grain. Here red is verification data, green Boxscan data and yellow is overlap. The pixel size is 2 micrometers.

where the ART was used for reconstructing the 3D grain shape, 87% of the grains voxels were assigned correctly compared to the verification data. This indicates that the use of the additional projection information gives similar results even without information about neighbouring grains.

Since grains are positioned in a spacefilling network and thus are further constrained, it may be possible to improve the grain shape reconstruction even further by using this knowledge. In other words, the current result from ART reconstruction may be improved by extending the ART implementation to simultaneously solve the 3D grain shape of a number of grains, or by combining the output of the ART reconstruction with a Monte Carlo scheme where the shape of a number of grains are refined simultaneously by a forward simulation. Another and maybe more obvious way to improve the result would be to vary the experimental settings. Extending the ω -range such that more projections are measured or decreasing the step sizes δ_y and δ_z could also improve the result.

6. CONCLUSIONS

A method for reconstructing the 3D shape of single grains from Boxscan data was described, implemented and applied to a dataset. Comparison of the reconstructed 3D shape to verification data showed that the reconstruction was smoother and more rounded than the verification data. Despite the smoothing, it is possible to reconstruct the grain with an average error of 2.7 micrometers on the location of the grain boundary.

ACKNOWLEDGEMENT

EML, AL, and RWF gratefully acknowledge funding for this program by the Office of Naval Research as part of the Dynamic 3-D Digital Structure Program under Grant Nos. N00014-05-WX-2-0555 and N00014-05-WX-2-0116 (Dr. J. Christodoulou, program manager). AL,

AA, HOS, SRD and EML furthermore acknowledges the Danish National Research Foundation for supporting the Center for Fundamental Research: Metal Structures in 4D, within which part of this work was performed. The provision of beam time by the ESRF, Grenoble, France, is greatly acknowledged. Furthermore, the staff at Risø-DTU thanks R. Gardner for valuable discussions.

REFERENCES

- Alpers, A., Poulsen, H.F., Knudsen, E., and Herman, G.T. (2006). A discrete tomography algorithm for improving the quality of 3DXRD grain maps. *J. Appl. Cryst.*, **39** 582-588.
- Cloetens, P., Ludwig, W., Baruchel, J., Guigay, J.P., Pernot-Rejmankova, P., Salome-Pateyron, M., Schlenker, M., Buffiere, J.Y., Maire, E. and Peix, G. (1999). Hard x-ray phase imaging using simple propagation of a coherent synchrotron radiation beam. *J. Phys. D: Appl. Phys.* **32** A145A151.
- Fu, X., Knudsen, E., Poulsen, H.F., Herman, G.T., Carvalho, B.M. and Liao H.Y. (2006). Optimized algebraic reconstruction technique for generation of grain maps based on three-dimensional x-ray diffraction (3DXRD). *Opt. Eng.* **45** 116501-1.
- Johnson, G., King, A., Honnicke, M.G., Marrow, J. and Ludwig, W. (2008). X-ray diffraction contrast tomography: a novel technique for three-dimensional grain mapping of polycrystals. II. The combined case. *J. Appl. Cryst.* **41** 310-318.
- Kak, C.A. and Slaney, M. (1988). Principles of computerized tomographic imaging (IEEE Press, New York).
- Lauridsen, E.M., Schmidt, S., Suter, R.M. and Poulsen, H.F. (2001). Tracking: a method for structural characterization of grains in powders or polycrystals. *J. Appl. Cryst.* **34** 744-750.
- Ludwig, W., Schmidt, S., Lauridsen, E.M. and Poulsen, H.F. (2008). X-ray diffraction contrast tomography: a novel technique for three-dimensional grain mapping of polycrystals. I. Direct beam case. *J. Appl. Cryst.* **41** 302-309.
- Ludwig, W., Reischig, P., King, A., Herbig, M., Lauridsen, E.M., Johnson, G., Marrow, T.J., and Buffiere, J.Y. (2009). Three-dimensional grain mapping by X-ray diffraction contrast tomography and the use of Friedel pairs in diffraction data analysis. *Rev. Sci. Instr.* **80** 033905-9.
- Lyckegaard, A., Lauridsen, E.M., Ludwig, W., Fonda, R.W. and Poulsen, H.F. (2010a) On the use of Laguerre tessellations for representations of 3D grain structures. *Adv. Eng. Mat.* Accepted.
- Lyckegaard, A., Poulsen, H.F., Ludwig, W., Fonda, R.W., Margulies, L., Götz, A., Sørensen, H.O., Dey, S.R. and Lauridsen, E.M (2010b). Boxscan: A novel 3DXRD-based method for mapping of polycrystalline materials. In preparation.
- Morawiec, A. and Field, D.P. (1996). Rodrigues parametrization for orientation and mis-orientation distributions. *Philos. Mag.* **73**. 1113-1130.
- Oddershede, J., Schmidt, S., Poulsen, H.F., Sørensen, H.O., Wright, J. and Reimers, W. (2010). Determining grain resolved stresses in polycrystalline materials using three-dimensional X-ray diffraction. *J. Appl. Cryst* **43** 539-549.
- Poulsen, H.F and Fu, X. (2003). Generation of grain maps by an algebraic reconstruction technique. *J. Appl. Cryst.* **36** 1062-1068.
- Poulsen, H.F (2004). Three-dimensional X-ray diffraction microscopy (Springer, New York).
- Suter, R.M., Hennessy D., Xiao, C. and Lienert, U. (2006). Forward modelling method for microstructural reconstruction using x-ray diffraction microscopy: Single-crystal verification. *Rev. Sci. Instr.* **77** 123905-1.